

Carbonate apatite versus β -tricalcium phosphate for rat vertical bone augmentation: A comparison of bioresorbable bone substitutes using polytetrafluoroethylene tubes

Makiko YANO¹, Kenichirou YASUI¹, Jun-ichiro JO², Aki NISHIURA¹, Yoshiya HASHIMOTO² and Naoyuki MATSUMOTO¹

¹Department of Orthodontics, Osaka Dental University, 8-1 Kuzuhahanazono-cho, Hirakata, Osaka 573-1121, Japan

²Department of Biomaterials, Osaka Dental University, 8-1 Kuzuhahanazono-cho, Hirakata, Osaka 573-1121, Japan

Corresponding author, Kenichirou YASUI; E-mail: yasui-k@cc.osaka-dent.ac.jp

This study radiologically and histologically compared two bioresorbable bone substitutes with different compositions carbonate apatite (Cytrans® Granules; CGs) and β -tricalcium phosphate (β -TCP) for vertical bone augmentation on a rat skull using a polytetrafluoroethylene (PTFE) tubes. This PTFE tube was placed at the center of the skull, fixed with Super Bond, and augmented with CGs or β -TCP granules. Specimens with surrounding tissue were harvested at 4, 8, and 12 weeks postoperatively, and radiological and histological evaluations were performed. The bone volume to total volume ratio (BV/TV) of the β -TCP-implanted group was markedly higher than that of the CG-implanted group at 4 and 12 weeks postoperatively. Compared to CGs, β -TCP exhibited the ability to form blood vessels into the graft material for a short period after transplantation, as well as an elevated production of collagen into β -TCP granules during the bone formation process.

Keywords: β -tricalcium phosphate, Carbonate apatite, Picrosirius red staining, VWF immunostaining, Vertical bone augmentation

INTRODUCTION

Inducing new bone formation in the jawbone has enabled the clinical performance of oral implants and orthodontic treatments. Effective vertical bone augmentation is particularly beneficial for patients with alveolar bone loss¹⁾. Autogenous bone grafting has conventionally been used for bone augmentation, but in recent years, the development of new, less invasive artificial bone replacement materials has gained traction as an alternative to autogenous bone²⁻⁴⁾. In organic components, such as calcium phosphate and calcium carbonate found in human bones, have emerged as potential candidates for artificial bone replacement materials^{5,6)}.

β -tricalcium phosphate (β -TCP) is a bioceramic with high biosafety. As a component of the bone matrix⁷⁾, β -TCP is composed of phosphoric acid and calcium bound together⁸⁾. It has a porous structure and is in the low-temperature stable phase among calcium phosphates³⁾. Over time, β -TCP is absorbed into the bone and gradually replaced by new bone until complete substitution occurs³⁾.

Cytrans® Granules (CGs) are artificially synthesized from low-crystalline carbonate apatite through a dissolution–precipitation reaction using calcium carbonate, calcium hydrogen phosphate, and calcium sulfate as precursor materials; without undergoing a sintering process⁹⁾. Carbonate apatite granules are osteoclast-resorbable¹⁰⁾ and are replaced by bone, akin to autologous bone⁵⁾. Additionally, they exhibit excellent osteoconductive properties¹¹⁾. Since their commercial launch in 2018, CGs have found widespread application in clinical practice. Their use includes maxillary sinus floor elevation, alveolar crest creation, application for

bone loss following the removal of jaw cysts, periodontal disease, and jawbone reconstruction and regenerative medicine^{5,9)}. The technique has been expanded to address a variety of applications.

In dentistry, bone strength and regenerated bone volume are crucial for the development of bone regenerative medicine due to the presence of occlusal forces and other loads⁸⁾. Bone strength comprises two parameters: bone density and bone quality. The quality of newly formed bone can be evaluated based on the degree of collagen maturation¹²⁾. Further, successful bone regeneration necessitates proper blood supply and circulation through newly formed blood vessels. Bone density indicates the amount of minerals per unit area and volume of bone. Although many studies have examined the effects of bioresorbable bone substitutes, including carbonate apatite and β -TCP, on bone density, few have focused on bone quality.

Although bone healing has been demonstrated in animal models of bone defect¹³⁻¹⁵⁾ and maxillary sinus surgery¹⁶⁾, few studies have been conducted on vertical bone augmentation. We aim to elucidate the mechanism underlying the bone augmentation process by evaluating collagen maturation and angiogenesis in the new bone using the bioresorbable bone substitutes carbonate apatite and β -TCP to provide a novel animal model for investigating bone augmentation in vertical bone defects, with potential for future treatment using bioresorbable bone substitutes.

MATERIALS AND METHODS

Material preparation

Granular β -TCP (Taihei Chemical Industrial, Osaka,

Japan) with a particle size of 500–1,700 μm was ground in a mortar, and particles were collected using a sieve with 500 μm pores, followed by another sieve with 100 μm pores to collect the β -TCP that remained. This method was used to adjust β -TCP to a size range of approximately 500 μm . CGs (GC, Tokyo, Japan) with S size granules (300–600 μm in diameter) and polytetrafluoroethylene (PTFE) tubes (Osaka Yakken, Osaka, Japan) were used in this experiment.

Characterization of β -TCP and CGs

The CGs and β -TCP granules were coated with osmium using an HPC-20 osmium coater (Vacuum Device, Ibaraki, Japan) and observed using a scanning electron microscope (SEM; S-4800; Hitachi High-Tech, Tokyo, Japan) after conductivity treatment. The crystal structures of β -TCP and CGs were analyzed using X-ray diffraction analysis (XRD-6000, Shimadzu, Kyoto, Japan) with Cu K α radiation at 40 kV and 30 mA. The scanning speed was 2°/min, and the 2 θ range was 10°–70°. Chemical bonding in β -TCP and CGs was analyzed using ATR-FTIR (IRAffinity-1S, Shimadzu) with a range of wavenumbers from 400 to 2,500 cm^{-1} and 16 scans.

Experimental animals

Thirty-six 8-week-old male Sprague–Dawley (SD) rats weighing 250–270 g (Shimizu Laboratory Supplies, Kyoto, Japan) were used for this experiment. The rats were housed in a rearing environment of 20°C and 50% humidity and were fed a solid diet, with drinking water supplied automatically from the tap. Thirty-six rats were divided into the following 3 groups of 12 rats each: β -TCP-implanted group; CG-implanted group; and a group implanted with PTFE tubes only. Animal experiments were conducted in accordance with the animal experimental regulations of Osaka Dental University after obtaining approval from the Animal Experiment Committee of Osaka Dental University (approval numbers: 21-02006, 22-02003, and 23-01002).

Transplantation method

The anesthesia protocol for the rats involved intraperitoneal injection of a combination of medetomidine (DOMITOL®, NIPPON ZENYAKU KOGYO, Fukushima, Japan), midazolam (Sandoz, Sandoz Pharma, Tokyo, Japan), and butorphanol tartrate (Betrufal®, Meiji Seika Pharma, Tokyo, Japan) to induce a general anesthetic. After shaving with an electric animal hair clipper and hair removal with a hair removal cream, local anesthesia with lidocaine (Xylocaine® 2%, Sandoz Pharma) was administered. The scalp was incised with a Feather Disposable Scalpel (No.15, Feather Safety Razor, Osaka, Japan). After full-layer valve formation, a PTFE tube (dimensions, 7-mm outer diameter, 5-mm inner diameter, and 2.5-mm height) was placed in the center of the skull and fixed with Super Bond (FF2068, Sun Medical, Shiga, Japan) by bonding the outer circumference of the tube and the joint (Figs. 1A and 2). A 4-0 polyamide Suture (699G, Johnson & Johnson, Tokyo, Japan) was used

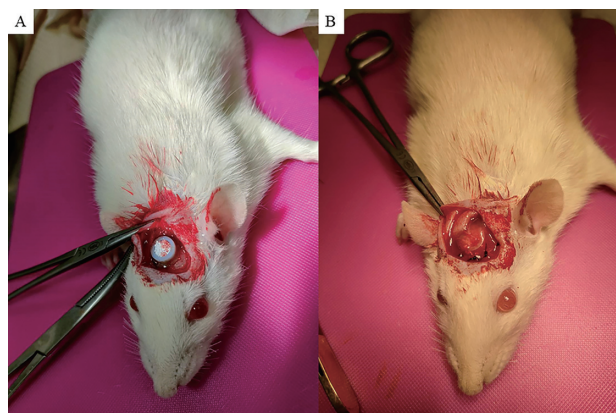


Fig. 1 (A) Photograph of rat skull after implantation of PTFE tube and material.
(B) Photograph of rat after periosteal suture.

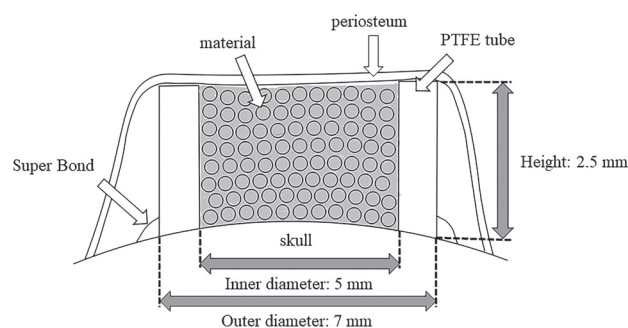


Fig. 2 Schematic of rat skull in sagittal section after material grafting.

to suture the periosteum (Fig. 1B). After the surgery, the head was closed with 4-0 polyamide suture. To prevent infection, an antibacterial drug (penicillin G, 22 units/g) was administered intramuscularly for 3 days postoperatively. The rats were carefully monitored for any signs of feeding difficulty, abnormal posture, respiratory disturbance, rapid weight loss (more than 20% in a few days) or any other symptoms of anguish. If any such symptoms occurred, a humane endpoint was applied, and the experiment was terminated with euthanasia by intraperitoneal overdose of barbiturates. The PTFE tubes used in the study had an outer diameter of 7 mm, inner diameter of 5 mm, and height of 2.5 mm (Fig. 2). The rats were divided into three groups of 12 rats each. β -TCP and PTFE tubes were dry-heat sterilized at 180° for 2 h and at 170° for 1 h, respectively, in a dry-heat sterilizer (KM-300B-R, AS ONE, Osaka, Japan). The experimental groups received β -TCP or CG implants. The control group was only implanted with PTFE tubes at 4, 8, and 12 weeks. Four rats in each group were euthanized by an intraperitoneal overdose of barbiturates, and the cranial crown was removed for further analysis.

Microfocus X-ray CT analysis

The skulls of the rats underwent microfocus X-ray CT imaging (SKY SCAN1275, Shimadzu) with a tube voltage of 65 kV and current of 85 μ A. Three-dimensional CT images were obtained using CTvox (BRUKER, Kanagawa, Japan) to observe the grafted material and new bone in the sagittal plane of the experimental and control groups. Quantitative measurement of new bone in the PTFE tube was performed using CTAn (BRUKER) after microfocus X-ray CT imaging. Calibration of bone mineral density (BMD) values was performed using a RATOC phantom. Calibration curves were prepared by measuring the attenuation coefficient values of each disk with seven different BMD values, and the slope and intercept were entered into CTAn for calibration. Forty layered shots per specimen were obtained. The volume inside the tube was measured to determine the total volume (TV, cm^3) and bone volume (BV, cm^3), and the bone volume to total volume ratio (BV/TV, %) was calculated. The results of each experimental group were compared based on these calculated results.

Picrosirius red staining

The removed rat skulls were cut into two sections at the center sagittal section using a diamond band saw (BS-3000, EXAKT, Norderstedt, Germany). The sections were then fixed in 4% paraformaldehyde–phosphate buffer (Nacalai Tesque, Kyoto, Japan) at 4°C for 3 days and subsequently decalcified in a 10% EDTA solution for 1 week before embedding in paraffin to prepare a paraffin block. A sagittal section of the skull graft site was prepared by thinning it to 3 μm in the sagittal plane. Picrosirius red staining was performed according to standard protocols, and morphological observations were made using an HS all-in-one fluorescence microscope (BZ-9000, KEYENCE, Osaka, Japan) to evaluate the new bone tissue in the PTFE tube and the mechanics of bone growth. Type I and type III collagen in the PTFE tubes were observed using polarized light microscopy (ECLIPSE Ci-POL, Nikon Solutions, Tokyo, Japan) after Picrosirius red staining to evaluate bone quality.

Immunohistochemical observation

Rat skulls were fixed in a 4% paraformaldehyde–phosphate buffer solution for 3 days at 4°C. After fixation, the samples were frozen and embedded in dry ice, hexane (FUJIFILM, Osaka, Japan), a special cryoembedding agent (SCEM, Leica Camera Japan, Tokyo, Japan), and an embedding device using the Kawamoto method. The frozen sections were cut into 5- μm thin slices using a high-function cryostat for research (CM 3050S, Leica Camera Japan). For von Willebrand Factor (vWF) staining, frozen sections were first cold air-dried, treated with Dako Proteinase K (S3020, Agilent Technologies, Santa Clara, CA, USA) for activation, then immersed in a 3% hydrogen peroxide solution using 30% hydrogen peroxide (081-04215, FUJIFILM Wako Pure Chemical), and blocked with Dako Protein blocking agent (X0909, Agilent Technologies) for 60 s. The primary antibody anti-vWF

(ab6994, Abcam, Cambridge, UK) was used at a dilution of 1:2000 for 60 s, followed by secondary antibody Dako HRP Labelled anti-rabbit (K4003, Agilent Technologies) for 60 s, and Dako DAB substrate and buffer (K3468, Agilent Technologies), followed by nuclear staining with Meyer's hematoxylin, dehydration, permeabilization, and encapsulation. Finally, blood vessels were observed after vWF staining using an HS all-in-one fluorescence microscope (BZ-9000, KEYENCE). On the images, the number of blood vessels in the area inside the PTFE tube was measured using ImageJ software (Version 1.54d, National Institutes of Health, Bethesda, MD, USA).

Statistical analysis

The experimental data was statistically analyzed using the multiple comparison and Tukey–Kramer methods. The calculations were made using a significance level of 1% and 5%, and differences were considered statistically significant if the *p*-value was less than 0.05.

RESULTS

Physicochemical characterization

The SEM images of β -TCP and CGs are presented in Fig. 3, revealing porous structures in both granule types. The granule surface of the CGs was smoother with a finer porous structure compared to β -TCP granules. Figure 4 shows the XRD analysis of β -TCP and CGs, with the X-ray diffraction spectra obtained from the JCPDS data. β -TCP showed a peak for β -TCP (JCPDS File No. 00-009-0169), and CGs showed a peak for carbonate apatite (JCPDS File No. 00-009-0432). Broad peaks in CGs indicate low crystallinity^{11,17-19}. The FTIR analysis of β -TCP and CGs are shown in Fig. 5. The FTIR spectrum

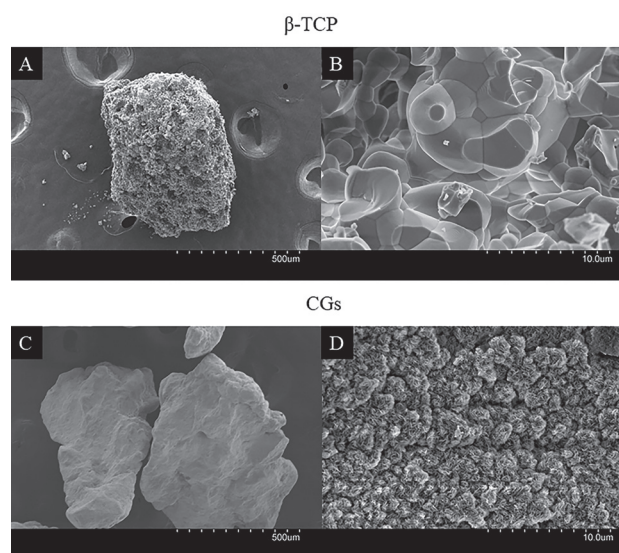


Fig. 3 SEM images of β -TCP [(A) and (B)] and Cytrans® Granules (CGs) [(C) and (D)]. left: low magnification ($\times 100$), right: high magnification ($\times 5,000$). Scale bars: (A) and (C), 500 μm ; (B) and (D), 10 μm .

of β -TCP showed phosphate ion peaks at 1001, 603, and 540 cm^{-1} , whereas the CGs exhibit carbonate ion peaks at 1471, 1411, and 871 cm^{-1} (11,18,20,21).

Microfocus X-ray CT analysis

The sagittal CTvox images of the control group, the β -TCP-implanted group, and the CG-implanted group are compared in this study. In the control group, new bone growth was observed on the inner wall side of the tube over 8 weeks postoperatively (Figs. 6A–C). β -TCP granules were found to fill the tube at 4 weeks postoperatively (Fig. 6D). In the CG-implanted group, the total volume decreased owing to the absorption of CG at 12 weeks postoperatively, and new bone formation was confirmed on the inner wall of the tube over time (Figs. 6G–I).

The results of the statistical analysis are shown in Fig. 7. In the BV/TV analysis, the β -TCP-implanted group had higher BV/TV values than the CG-implanted group at 4 weeks postoperatively, with both groups having

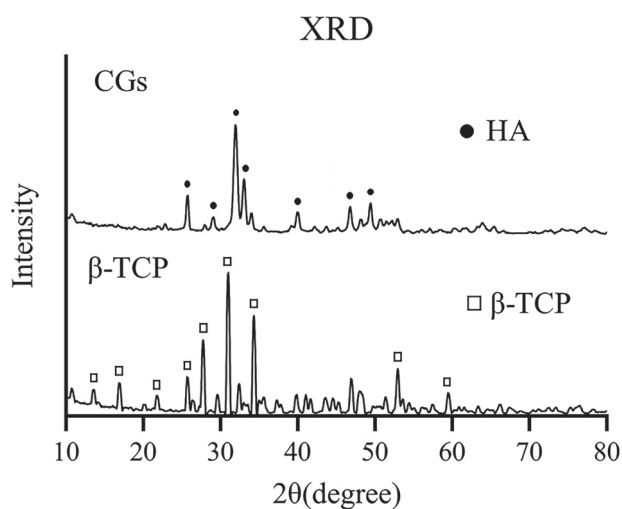


Fig. 4 XRD patterns of β -TCP and Cytrans® Granules (CGs).

● represents the pattern of hydroxyapatite (HA). □ represents the pattern of β -TCP.

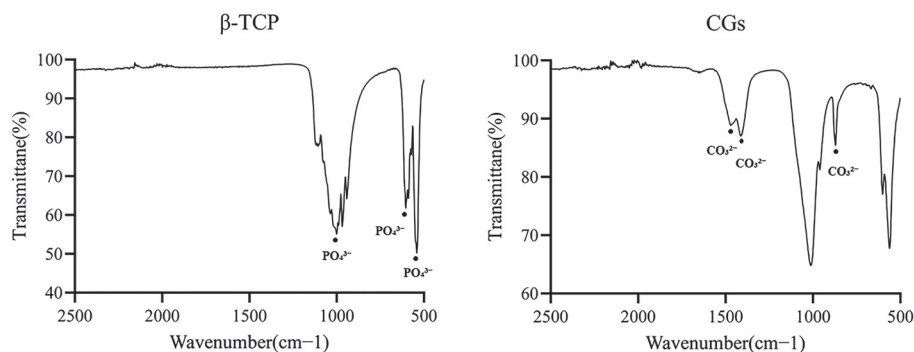


Fig. 5 FT-IR spectrum of β -TCP and Cytrans® Granules (CGs).

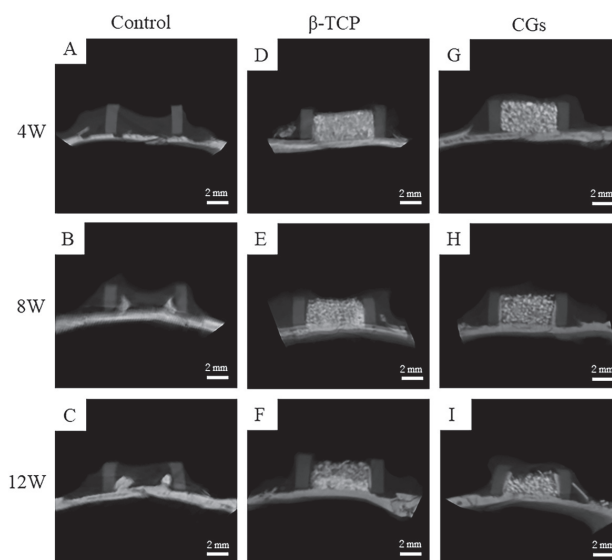


Fig. 6 Microfocus X-ray CT images at 4, 8, and 12 weeks postoperatively implanted group.

Control group is (A), (B), and (C). β -TCP-implanted group is (D), (E), and (F). Cytrans® Granule (CG)-implanted group is (G), (H), and (I). Scale bars: 2 mm.

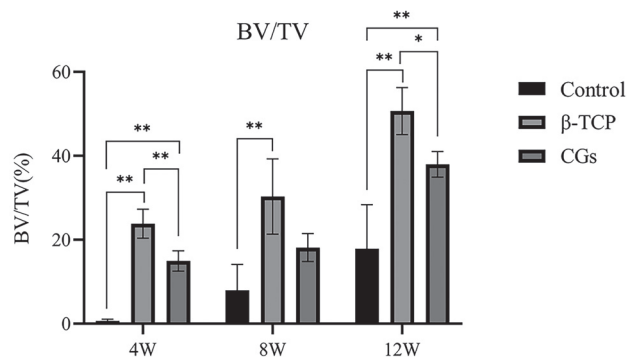


Fig. 7 Bone volume fraction (BV/TV) analysis for each group at 4, 8, and 12 weeks postoperatively.

** indicates a p -value of less than 0.01, * indicates a p -value of less than 0.05.

significantly different values from the control group. At 8 and 12 weeks postoperatively, β -TCP continued to have higher values than CGs, and significant differences were observed between the material-implanted and control groups at all time points.

Picrosirius red staining

1. Four weeks postoperatively implanted group

An overall view under an all-in-one fluorescence microscope with picrosirius red staining is shown in Fig. 8. In the control group, no tissue was detected inside the PTFE tubes (Fig. 8A), while in the β -TCP-implanted group, the tube was filled with β -TCP granules (Fig. 8D).

The CG-implanted group presented CGs with connective tissue between the granules (Fig. 8G). Both the β -TCP- and CG-implanted groups showed little bone-like tissue, and the graft material remained.

Picrosirius red staining under polarized light microscopy was used to evaluate collagen fiber thickness and maturity, with type I collagen appearing thick yellow, orange, or red; and type III collagen appearing thin and green (Figs. 9–11). In the control group, no collagen was found in the tubes (Figs. 9A–C). In the β -TCP-implanted group, the inside of the tube was mainly composed of type III collagen, with some type I collagen present (Figs. 10A–C). On the inner tube wall side, type I collagen was mainly expressed. In the CG-implanted group, type III collagen was also predominant 4 weeks postoperatively (Figs. 11A–C). The comparison between the β -TCP-implanted group and the CG-implanted group indicated that both presented mainly type III collagen.

2. Eight weeks postoperatively implanted group

The control group showed collagen accumulation along the inner tube wall at 8 weeks postoperatively under all-in-one fluorescence microscopy with picrosirius red staining (Fig. 8B). In the β -TCP-implanted group, collagen

started to appear from the basal bone side from 8 weeks postoperatively and β -TCP granules were being replaced by bone (Fig. 8E). In contrast, in the CG-implanted group, CGs were still present at 4 weeks postoperatively, and collagen accumulation was observed in the inner walls of the tubes (Fig. 8H). Images captured under polarized light microscopy with picrosirius red staining showed that type I and type III collagen appeared on the inner

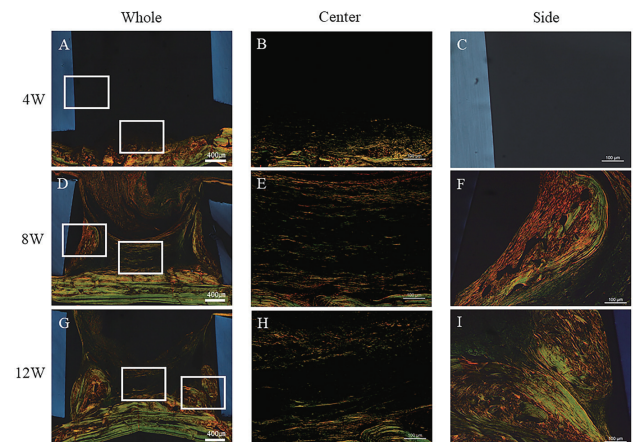


Fig. 9 Histological images as observed under polarized light microscopy of picrosirius red staining in the control group at 4, 8, and 12 weeks postoperatively. Whole PTFE tube images: (A), (D) and (G). Original magnification: $\times 4$. Scale bars: 400 μ m. PTFE tube center: (B), (E) and (H). PTFE tube inner wall side: (C), (F) and (I). Original magnification: $\times 10$. Scale bars: 100 μ m.

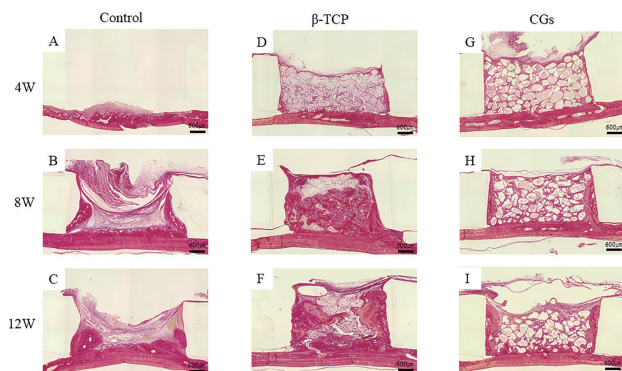


Fig. 8 Histological images observed with all-in-one fluorescence microscope of picrosirius red staining in each group at 4, 8, and 12 weeks postoperatively. Control group: (A), (B) and (C), β -TCP-implanted group: (D), (E), and (F), Cytrans[®] Granule (CG)-implanted group: (G), (H), and (I). Original magnification: $\times 4$. Scale bars: 600 μ m.

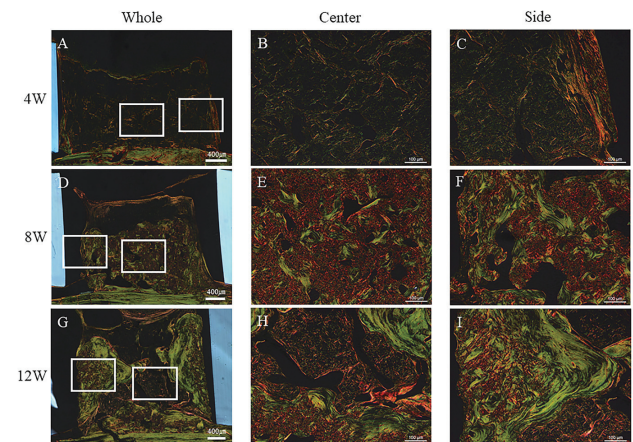


Fig. 10 Histological images observed under a polarized light microscopy of picrosirius red staining in the β -TCP-implanted group at 4, 8, and 12 weeks postoperatively. Whole PTFE tube: (A), (D) and (G). Original magnification: $\times 4$. Scale bars: 400 μ m. PTFE tube center: (B), (E) and (H). PTFE tube inner wall side: (C), (F) and (I). Original magnification: $\times 10$. Scale bars: 100 μ m.

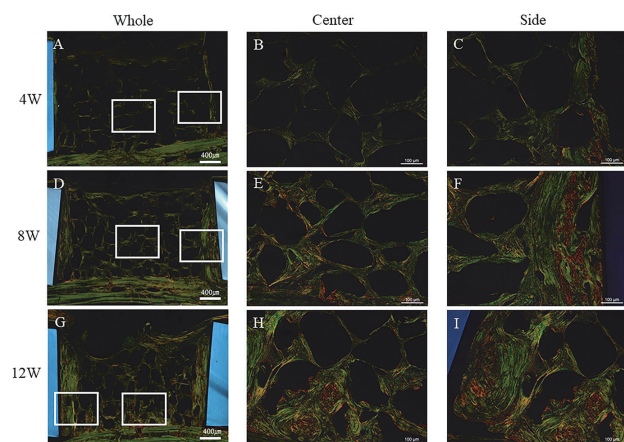


Fig. 11 Histological images observed under polarized light microscopy of picrosirius red staining in the Cytrans® Granule (CG)-implanted group at 4, 8, and 12 weeks postoperatively. Whole PTFE tube: (A), (D) and (G). Original magnification: $\times 4$. Scale bars: 400 μm . PTFE tube center: (B), (E) and (H). PTFE tube inner wall side: (C), (F) and (I). Original magnification: $\times 10$. Scale bars: 100 μm .

side wall of the tube at 8 weeks postoperatively in the control group; no collagen appeared inside the tube (Figs. 9D–F). In the β -TCP-implanted group, the inside of the tube contained a mixture of type I and type III collagen at 8 weeks postoperatively. Type I collagen was slightly more abundant and accumulated on the inner wall of the tube. At 8 weeks postoperatively, each collagen was clearly separated and distinguishable compared to 4 weeks postoperatively (Figs. 10D–F). In the CG-implanted group, the amount of collagen between the granules increased at 8 weeks postoperatively, with a mixture of type I and type III collagen present. Type I collagen was also found to accumulate on the inner wall of the tube (Figs. 11D–F). Comparing the β -TCP-implanted group with the CG-implanted group, type I collagen was more abundant in the β -TCP-implanted group. In addition, collagen was found to invade the β -TCP granules, but not the CGs.

3. Twelve weeks postoperatively implanted group

Observational images obtained under an all-in-one fluorescence microscope with picrosirius red staining demonstrated an increased amount of collagen on the basal bone surface at 12 weeks postoperatively in the control group, compared to that at 8 weeks postoperatively (Fig. 8C). In the β -TCP-implanted group, there was a further increase in the amount of collagen at 12 weeks postoperatively compared to at 8 weeks postoperatively (Fig. 8F). In the CG-implanted group, the CGs were still present at 4 and 8 weeks postoperatively (Fig. 8I). Increased collagen levels were observed on the inner walls of the tube. This confirmed that the amount of collagen on the inner side of the tube wall increased over

time. It was also observed that the carbonate apatite granules in the CG implant group were less angulated and were slightly smaller in size than those at 4 and 8 weeks postoperatively.

Comparing the β -TCP- and CG-implanted groups, collagen generation was observed from the inner wall of the tube and the basal bone surface in both groups, suggesting that the mode of new bone growth was similar. However, the β -TCP granules were replaced with bone, whereas the CGs could not be replaced by bone until 12 weeks postoperatively. Images captured under polarized light microscopy with picrosirius red staining showed that type I and type III collagen appeared on the inner wall of the tube at 8 weeks and 12 weeks postoperatively in the control group; no collagen appeared inside the tube (Figs. 9G–I). In the β -TCP-implanted group, the inside of the tube was mostly occupied by type I collagen (Figs. 10G–I). Layered collagen accumulation was observed on the inner tube wall. In the CGs, collagen did not penetrate the granules until 12 weeks postoperatively, and collagen expression was mainly observed in the intergranular space. In addition, an increased amount of type I collagen was observed in the intergranular area of CGs (Figs. 11G–I). Both the β -TCP-implanted group with the CG-implanted groups showed an increased appearance of type I collagen inside the PTFE tube, with type I collagen being predominant in the β -TCP group.

Immunohistochemical observation

1. Four weeks postoperatively implanted group

In vWF staining, blood vessels appeared brown, confirming angiogenesis. Figure 12 shows images of the control, β -TCP- and CG-implanted groups under an all-in-one fluorescence microscope. In the control group, few vessels could be observed at 4 weeks postoperatively (Fig. 12A). In the β -TCP-implanted group, numerous blood vessels were observed between the β -TCP granules at 4 weeks postoperatively (Fig. 12B). In the CG-implanted group, blood vessels were also observed between the CGs at 4 weeks postoperatively, but their number was lower than in the β -TCP-implanted group (Fig. 12C).

2. Eight weeks postoperatively implanted group

In the control group, some angiogenesis could be seen inside the tubes (Fig. 12D). In the β -TCP-implanted group, a significant number of blood vessels were observed between the β -TCP granules (Fig. 12E). As observed at 4 weeks postoperatively, numerous vessels were observed at 8 weeks postoperatively. In the CG-implanted group, some angiogenesis was observed between CGs (Fig. 12F), but the number of blood vessels was lower compared to the β -TCP-implanted group. The number of blood vessels slightly increased from 4 to 8 weeks postoperatively. Comparing the β -TCP-implanted group with the CG-implanted group, a higher number of blood vessels were observed in the β -TCP-implanted group, suggesting a more significant angiogenic response.

3. Twelve weeks postoperatively implanted group

In the control group, a large amount of angiogenesis

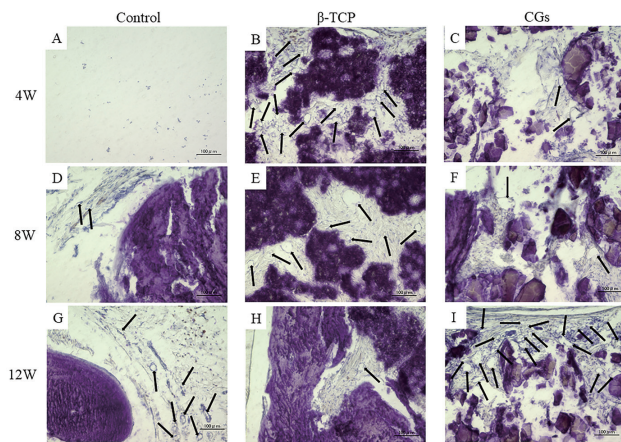


Fig. 12 Histological images of vWF-immunostained sections from the control, β -TCP-implanted, and Cytrans[®] Granule (CG)-implanted groups at 4, 8, and 12 weeks postoperatively. Original magnification: $\times 20$. Scale bars: 100 μ m.

could be observed inside the tube, and the number of vessels was higher at 12 weeks postoperatively than at 8 weeks postoperatively (Fig. 12G). In the β -TCP-implanted group, the number of blood vessels was lower at 12 weeks postoperatively than at 4 and 8 weeks postoperatively (Fig. 12H). Conversely in the CG-implanted group, numerous angiogenic events were still observed between CGs at 12 weeks postoperatively (Fig. 12I), with a significant increase in the number of blood vessels compared to that at 8 weeks postoperatively. Comparison of the β -TCP- and CG-implanted groups showed that angiogenesis in the β -TCP-implanted group began to decline after 12 weeks postoperatively, whereas in the CG-implanted group, angiogenesis remained active. These results suggest that blood vessel formation occurred earlier in the β -TCP-implanted group, with a subsequent decrease in the number of blood vessels after 12 weeks postoperatively compared to the CG-implanted group. Additionally, blood vessel formation was slower in the CG-implanted group than in the β -TCP-implanted group, with no reduction in the number of blood vessels observed after 12 weeks postoperatively.

Number of blood vessels by immunohistochemical observation

The number of blood vessels in each group is shown in Fig. 13. The β -TCP-implanted group had the highest number of blood vessels among all groups tested at 4 weeks postoperatively. At 8 weeks postoperatively, the β -TCP-implanted group had a higher number of blood vessels than the control group. At 12 weeks postoperatively, the β -TCP implanted groups had a lower number of vessels than the CG-implanted group.

DISCUSSION

We have developed a new, minimally invasive model

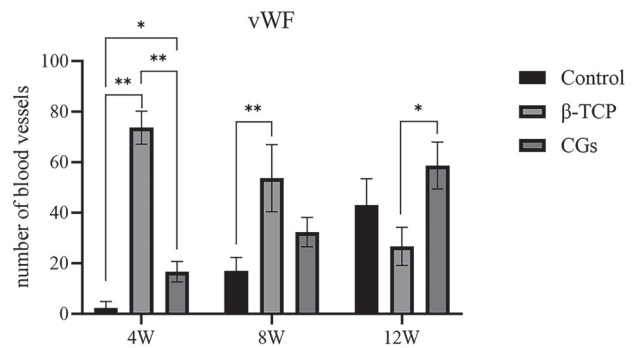


Fig. 13 Comparison of the overall number of vessels in the PTFE tube for each group at 4, 8, and 12 weeks postoperatively.

** indicates p -value < 0.01 , * indicates p -value < 0.05 .

for vertical bone augmentation in the rat skull using a PTFE tube. Our study shows that the bioresorbable bone substitutes, carbonate apatite and β -TCP significantly promote the formation of new vertical tissue in this model. Moreover, we found that the timing of the initiation of mature collagen formation and angiogenesis differ between carbonate apatite and β -TCP.

Various models for bone augmentation have been created for bone augmentation methods, including placing a titanium cap^{22,23} or a Teflon tube²⁴ on the skull of rats or rabbits to attempt bone augmentation. Previous studies have reported conflicting findings regarding the need for cortical perforation in guided bone regeneration^{22,23,25}. Some researchers argue that cortical perforation is not essential, while others report its necessity²⁶. To create a less invasive model of vertical bone augmentation of the rat skull, we used a PTFE tube without cortical bone perforation. Instead of forming a ring-shaped groove with a trephine bar²⁷, which is a noninvasive experimental method, we used Super Bond to firmly fix the PTFE tube onto the skull of the rats.

The geometrical properties of the augmented bone were obtained by simultaneously scanning the calibration phantom using Microfocus X-ray CT. In the control group, we observed a slight emergence of new bone from the basal bone and detected BV/TV values using Microfocus X-ray CT analysis. This finding suggests that a space covered by existing bone and periosteum exists and that new bone will appear if there is no connective tissue intrusion into the space. β -TCP showed a significantly higher BV/TV value than CG, indicating that β -TCP was absorbed faster than CG at all time points and was replaced by bone. Ishikawa *et al.*¹⁸ reported that *in vitro*, β -TCP granules exhibited much higher solubility and greater Ca^{2+} release at physiological pH 7.3 solution compared to carbonate apatite granules. Moreover, Fukuda *et al.*²⁸ found that *in vivo*, the percentage of remaining material was significantly higher in the compared to that in the β -TCP-implanted group in alveolar bone augmentation in beagle dogs at 24 weeks postoperatively. These findings are

consistent with the microfocus X-ray CT analysis in this study. In addition, although the sizes of β -TCP and CGs were unified, SEM observations revealed morphological differences. CGs lack any pore structures, whereas β -TCP contains micropores in the macropore walls of the granular structure. This difference in structure may affect resorption.

In this study, picrosirius red staining combined with polarized light microscopy revealed the mechanism underlying collagen formation during new bone formation. The use of polarized light microscopy allowed for the differentiation of type I collagen (appearing yellow to red) from type III collagen (green), as well as the determination of collagen fiber thickness and maturity based on this color difference^{8,29,30}. In the β -TCP-implanted group, type III collagen was dominant at 4 weeks post-surgery, infiltrating the granules, but gradually transitioned to type I collagen over time. Twelve weeks post-surgery, type I collagen largely replaced type III collagen. This suggests that β -TCP granules were replaced by new bone from the basal bone side, with collagen maturation resulting in granule flattening and size reduction. No collagen invasion was observed in the CG group. Additionally, from 8 to 12 weeks post-surgery an increase in type I collagen was observed in the intergranular space, which subsequently transformed into new bone. Our findings are consistent with those of Gay *et al.*³¹, who reported that type III collagen appears first, followed by type I collagen, during the wound healing process in connective tissues.

Angiogenesis is crucial for bone augmentation, as it activates osteoclasts and osteoblasts. The differentiation of mesenchymal stem cells into blood vessels through the action of vascular endothelial growth factor is essential for osteogenesis⁶. In our study, many blood vessels appeared around β -TCP at 4 weeks postoperatively, and their number increased at 8 weeks, suggesting that β -TCP induces early blood vessel formation. Conversely, the highest number of blood vessels around the CGs was the highest at 12 weeks postoperatively. The presence of blood vessels is believed to promote the induction of osteoblasts and osteoclasts. Both materials showed vWF-positive blood vessels, likely due to blood flow and an abundant supply of nutrients resulting from the angiogenic process. In the initial stages, angiogenesis occurs, and as granules resorb and shrink, new bone and blood vessel rearrangements may occur, eventually leading to normal bone structure. Therefore, from a microcirculatory perspective, resorbable materials are useful for bone augmentation therapy, in addition to their importance in blood vessel formation.

In conclusion, the presented results indicate that the β -TCP demonstrated the ability to form blood vessels into the graft material for a short period after transplantation compared to that in CGs, as well as an elevated production of collagen into β -TCP granules during the bone formation process compared to that in CGs, using a new, less invasive model of vertical bone augmentation on rat skull. However, β -TCP is highly soluble under physiological conditions, as β -TCP

dissolution occurs mainly by hydrolytic degradation, despite exhibiting osteoclast resorption³². Fukuda *et al.*²⁸ demonstrated that a significantly higher percentage of new bone and bone-to-implant contact ratio was maintained in CGs compared to those in β -TCP at 24 weeks postoperatively through alveolar bone augmentation with simultaneous titanium implant placement in beagle dogs. However, long-term studies using this model are still necessary to fully evaluate the efficacy of β -TCP in bone augmentation.

ACKNOWLEDGMENTS

We express our sincere gratitude to Dr Masayasu Tatsumura and Dr Takeryo Adachi of the Department of Orthodontics, Osaka Dental University, Japan, for their assistance in performing the animal experiments and to Dr Kaoru Kusano of the Department of Oral Implantology, Osaka Dental University, Japan for their advice and support in the histological analysis. This work was supported in part by JSPS KAKENHI (grants 20K10240 and 22K10047).

REFERENCES

- 1) Urban IA, Montero E, Monje A, Sanz-Sánchez I. Effectiveness of vertical ridge augmentation interventions: A systematic review and meta-analysis. *J Clin Periodontol* 2019; 46: 319–339.
- 2) Arima Y, Uemura N, Hashimoto Y, Baba S, Matsumoto N. Evaluation of bone regeneration by porous alpha-tricalcium phosphate/atelocollagen sponge composite in rat calvarial defects. *Orthod Waves* 2013; 72: 23–29.
- 3) Matsuno T, Nakamura T, Kuremoto K, Notazawa S, Nakahara T, Hashimoto Y, *et al.* Development of beta-tricalcium phosphate/collagen sponge composite for bone regeneration. *Dent Mater J* 2006; 25: 138–144.
- 4) Sakai K, Hashimoto Y, Baba S, Nishiura A, Matsumoto N. Effects on bone regeneration when collagen model polypeptides are combined with various sizes of alpha-tricalcium phosphate particles. *Dent Mater J* 2011; 30: 913–922.
- 5) Ishikawa K. Carbonate apatite bone replacement: Learn from the bone. *J Ceram Soc Jpn* 2019; 127: 595–601.
- 6) Sato N, Handa K, Venkataiah VS, Hasegawa T, Njuguna MM, Yahata Y, *et al.* Comparison of the vertical bone defect healing abilities of carbonate apatite, β -tricalcium phosphate, hydroxyapatite and bovine-derived heterogeneous bone. *Dent Mater J* 2020; 39: 309–318.
- 7) Murakami S, Miyaji H, Nishida E, Kawamoto K, Miyata S, Takita H, *et al.* Dose effects of beta-tricalcium phosphate nanoparticles on biocompatibility and bone conductive ability of three-dimensional collagen scaffolds. *Dent Mater J* 2017; 36: 573–583.
- 8) Tatusumura M, Yasui K, Hashimoto Y, Matsumoto N. Elucidation of the mechanism of bone regeneration when a mixture of β -TCP and autologous bone granules are transplanted. *Nano Biomed* 2020; 12: 89–100.
- 9) Ishikawa K, Matsuya S, Lin X, Lei Z, Yuasa T, Miyamoto Y. Fabrication of low crystalline B-type carbonate apatite block from low crystalline calcite block. *J Ceram Soc Jpn* 2010; 118: 341–344.
- 10) Zhang X, Atsuta I, Narimatsu I, Ueda N, Takahashi R, Egashira Y, *et al.* Replacement process of carbonate apatite by alveolar bone in a rat extraction socket. *Materials* 2021;

- 14: 4457.
- 11) Akita K, Fukuda N, Kamada K, Kudoh K, Kurio N, Tsuru K, *et al.* Fabrication of porous carbonate apatite granules using microfiber and its histological evaluations in rabbit calvarial bone defects. *J Biomed Mater Res A* 2020; 108: 709-721.
- 12) Honda Y, Huang A, Zhao J, Han X, Kurushima Y, Gong Y, *et al.* Sustained release of catechin from gelatin and its effect on bone formation in critical sized defects in rat calvaria. *J Hard Tissue Biol* 2020; 29: 77-84.
- 13) Hieda A, Uemura N, Hashimoto Y, Toda I, Baba S. In vivo bioactivity of porous polyetheretherketone with a foamed surface. *Dent Mater J* 2017; 36: 222-229.
- 14) Tsumano N, Kubo H, Imataki R, Honda Y, Hashimoto Y, Nakajima M. Bone regeneration by dedifferentiated fat cells using composite sponge of alfa-tricalcium phosphate and gelatin in a rat calvarial defect model. *Appl Sci* 2021; 11: 11941.
- 15) Zhang Y, Jo JI, Chen L, Hontsu S, Hashimoto Y. Effect of hydroxyapatite coating by Er: YAG pulsed laser deposition on the bone formation efficacy by polycaprolactone porous scaffold. *Int J Mol Sci* 2022; 23: 9048.
- 16) Rong Q, Li X, Chen S, Zhu S, Huang D. Effect of the Schneiderian membrane on the formation of bone after lifting the floor of the maxillary sinus: An experimental study in dogs. *Br J Oral Maxillofac Surg* 2015; 53: 607-612.
- 17) Bui X, Thang TD. Synthesis of biphasic calcium phosphate and its behaviour in simulated body fluid. *AJSTD* 2016; 33: 63-68.
- 18) Ishikawa K, Miyamoto Y, Tsuchiya A, Hayashi K, Tsuru K, Ohe G. Physical and histological comparison of hydroxyapatite, carbonate apatite, and β -tricalcium phosphate bone substitutes. *Materials (Basel)* 2018; 11: 1993.
- 19) Wang F, Nakata H, Sun X, Maung WM, Sato M, Kon K, *et al.* A novel hydroxyapatite fiber material for the regeneration of critical-sized rabbit calvaria defects. *Dent Mater J* 2021; 40: 964-971.
- 20) Bhardwaj U, Sura R, Papadimitrakopoulos F, Burgess D. Controlling acute inflammation with fast releasing dexamethasone-PLGA microsphere/PVA hydrogel composites for implantable devices. *J Diabetes Sci Tech* 2007; 1: 8-17.
- 21) Kudoh K, Fukuda N, Akita K, Kudoh T, Takamaru N, Kurio N, *et al.* Reconstruction of rabbit mandibular bone defects using carbonate apatite honeycomb blocks with an interconnected porous structure. *J Mater Sci Mater Med* 2023; 34: 1-11.
- 22) Lundgren AK, Lundgren D, Hämmerle CH, Nyman S, Sennerby L. Influence of decortication of the donor bone on guided bone augmentation: An experimental study in the rabbit skull bone. *Clin Oral Implants Res* 2000; 11: 99-106.
- 23) Slotte C, Lundgren D. Impact of cortical perforations of contiguous donor bone in a guided bone augmentation procedure: an experimental study in the rabbit skull. *Clin Implant Dent Relat Res* 2002; 4: 1-10.
- 24) Takiguchi S, Kuboyama N, Kuyama K, Yamamoto H, Kondoh T. Experimental study of bone formation ability with the periosteum on rat calvaria. *J Hard Tissue Biol* 2009; 18: 149-160.
- 25) Rompen EH, Biewer R, Vanheusden A, Zahedi S, Nusgens B. The influence of cortical perforations and of space filling with peripheral blood on the kinetics of guided bone generation. A comparative histometric study in the rat. *Clin Oral Implants Res* 1999; 10: 85-94.
- 26) Hollier L. Bone augmentation osteogenesis using hydroxyapatite and beta-tricalcium phosphate blocks. *J Craniofac Surg* 2004; 15: 358-359.
- 27) Kostopoulos L, Karring T, Uraguchi R. Formation of jawbone tuberosities by guided tissue regeneration. An experimental study in the rat. *Clin Oral Implants Res* 1994; 5: 245-253.
- 28) Fukuda N, Kudoh K, Akita K, Takamaru N, Ishikawa K, Miyamoto Y. Comparison of bioresorbable bone substitutes, carbonate apatite and β -tricalcium phosphate, for alveolar bone augmentation with simultaneous implant placement. *Oral Sci Int* 2023; 20: 221-228.
- 29) Dahlin C, Sennerby L, Lekholm U, Linde A, Nyman S. Generation of new bone around titanium implants using a membrane technique: An experimental study in rabbits. *Int J Oral Maxillofac Implants* 1989; 4: 19-25.
- 30) Kaku M, Rosales Rocabado JM, Kitami M, Ida T, Akiba Y, Yamauchi M, *et al.* Mechanical loading stimulates expression of collagen cross-linking associated enzymes in periodontal ligament. *J Cell Physiol* 2016; 231: 926-933.
- 31) Gay S, Vijanto J, Raekallio J, Penttinen R. Collagen types in early phases of wound healing in children. *Acta Chir Scand* 1978; 144: 205-211.
- 32) Yamasaki N, Hirao M, Nanno K, Sugiyasu K, Tamai N, Hashimoto N, *et al.* A comparative assessment of synthetic ceramic bone substitutes with different composition and microstructure in rabbit femoral condyle model. *J Biomed Mater Res B* 2009; 91: 788-798.